Local dependent modelling of electric vehicle propulsion systems

Communication BI-6

Modèle de propulsion électrique pour véhicule en fonction de la charge.

Load dependent modelling of electric vehicle propulsion systems.

VAN DONGEN L.A.M., VAN DER GRAAF R., SCHOT J.A., VISSCHER W.H.M.
EINDHOVEN UNIVERSITY OF TECHNOLOGY
POB 513
NL-5600 MB EINDHOVEN
PAYS BAS

RESUME

Afin de pouvoir comparer et prédire la conduite d'un système de propulsion d'un véhicle électrique il est avantageux d'avoir un modèle de calcul a sa disposition. Ce programme doit être basée sur un modèle détaillé des systèmes de propulsion des véhicules électriques dependant du charge.
Les descriptions détaillées des caractéristiques de la batterie, du moteur à courant continu et la transmission mécanique font partie du modèle de calcul.
Transmission d'énergie à travers les organes de transmission pouvant être calculer a partir d'un cycle de charge dans laquelle la relation entre vitesse et temps est donné.
Il y a un bon concordement entre les calculs et les résultants expérimentals.

ABSTRACT

In order to predict and compare the behaviour of electric vehicle propulsion systems it is useful to have an accurate simulation program available. This program should be based on a detailed load dependent mathematical model of EV drive trains. In depth discriptions of the characteristics of battery, DC motor and mechanical transmission are used in this model.
Power flow through all parts of a drive line can accurately be calculated departing from a vehicle duty cycle, in which the speed versus time function is given.
Comparisons with measurements show a very good agreement.

Introduction

Since the energy and power density of energy storage systems for electric vehicles are still relatively small, development of drive systems has to be oriented to minimizing losses in and optimal matching of drive train components with respect to the energy consumption.
The efficiencies of drive train components strongly depend on the operating point.
The total amount of energy that can be delivered by a battery pack is determined by the driving cycle of the vehicle involved.
This paper is focussed on the matching of the various subsystems in an EV drive line.

A state of charge model for a lead-acid battery was determined. In this model the battery voltage was taken as a function of current and depth of discharge. It will appear that the battery pack and the DC-motor should be described as an integrated electric system. For this purpose equations were derived for each power loss mechanism associeted with the DC-motor. The total energy loss in the motor turns out to depend not only on the mechanical operating point but also on the battery state-of-charge.
The energy efficiency characteristics of the mechanical transmission are taken into account as a function of both torque and speed.

A detailed mathematical model of the total drive system was set up, in which the characteristics of the individual components are load dependent.
A digital computer simulation program based on this model has been written.
Simulation results are discussed in comparison with tests. It will be shown that the simulation program allows an accurated prediction of the power flow through the drive train components, including the battery and thus an accurate comparison of electric vehicle drives.

Model of the electric motor

A motor model, which describes the effciency purely as a function of torque and speed, is applicable only if an ideal voltage source is connected to the armature circuit. The voltage of a lead-acid battery however varies in dependence on the load and the state-of-charge. In the case of field current control, the armature voltage equals the battery voltage, so the field flux has to be adjusted during battery voltage variations if a certain mechanical operating point must be maintained. In field control therefore the armature and field current and consequently the motor efficiency depend not only on the mechanical operating point but also on the voltage-current-characteristics of the battery which on their turn depend on the state-of-charge of the battery.
A motor model, in which the total power loss is specified as a sum of component losses, is strongly recommended, in order that the effect of the battery voltage on the motor efficiency can be taken into account correctly.

The ideal separately excited DC-motor can be described by the following equations for motor torque (T) and voltage (V) resp.:

$$T = C_m * \Phi * I_a \qquad (1)$$

$$V = C_m * \Phi * \omega_m + R_a * I_a \qquad (2)$$

where C_m = motor constant
Φ = field flux
I_a = armature current
R_a = armature resistance
ω_m = angular speed of motor

The mechanical losses of a Siemens separately excited DC-motor, type 1GV1, have been determined as a function of speed by measuring the torque, which is required to rotate the armature at zero field current. These mechanical losses ($T_{l,mech}$), which include brush friction, windage and bearing friction, (see figure 1)

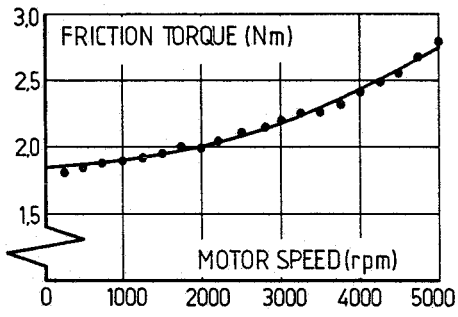

Fig. 1. Mechanical losses of DC-motor.

can be described by the formula:

$$T_{l,mech} = 3.108 * 10^{-6} * \omega_m^2 + 7.49 * 10^{-5} * \omega_m + 1.85 \qquad (3)$$

The iron losses (eddy current losses and hysteresis losses) are a function of field flux and motor speed. It is extremely difficult to predict the hysteresis and eddy current losses in a DC-motor theoretically because the shape of the magnetic field in the armature is not exactly known due to among other things armature reaction. The sum of the iron and the mechanical losses at zero armature current was experimentally determined.

From these results the following approximation of the iron losses ($T_{l,fe}$) was derived (figure 2):

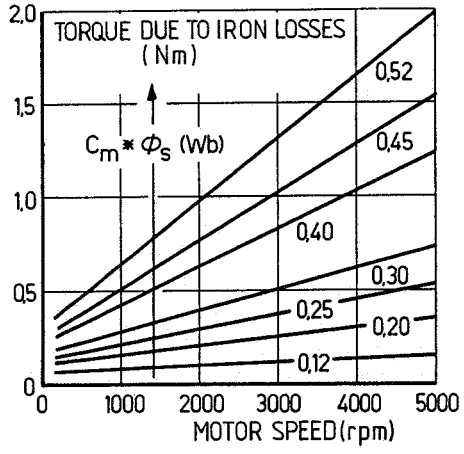

Fig. 2. Iron losses as a function of rotational speed and field flux.

$$T_{l,fe} = 0.55 * (C_m * \Phi) + 1.21 * 10^{-2} * (C_m * \Phi)^2 * \omega_m \quad (4)$$

The brush voltage drop depends on the type of brush being used. A positive voltage drop occurs during motor operation and a negative drop is used for regeneration. (See expression 8).
The voltage drop at one rotating brush-commutator-contact, V_{br}, amounts to 1.28 Volts. For an operating temperature of 115°C (following the VDE prescriptions) a value of 0.059 Ohm has been found for the total resistance of the armature circuit, R_a, and a value of 13.6 Ohm for the resistance of the field windings, R_f. The sum of the electric losses ($P_{l,el}$) can now be written as:

$$P_{l,el} = 2 * V_{br} * I_a + I_a^2 * R_a + I_f^2 * R_f \quad (5)$$

if the losses in the field chopper are neglected.
Due to magnetic saturation the field flux is not proportional to the field current.
This characteristic, indicated in figure 3, is

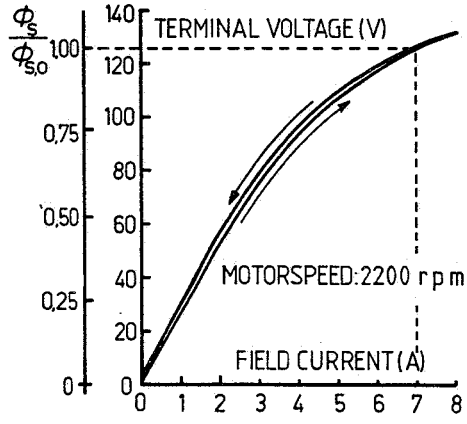

Fig. 3. Saturation curve of field flux.

similar to the "no-load-characteristics"which can be determined by recording the armature voltage as a function of the field current at nominal motor speed (2200 rpm). The nominal field current ($I_{f,0}$) of this motor stands at 7 Amps. With the help of equation $V = C_m * \Phi * \omega_m$ 0.545 Weber was found for the product of the machine constant (C_m) and the nominal field flux (Φ). For field currents lower than the nominal value the following expression can be applied:

$$\frac{C_m * \Phi}{C_m * I_o} = -1.441 * 10^{-2} * I_f^2 + 2.436 * 10^{-1} * I_f + 6.309 * 10^{-3} \quad (6)$$

Equations (1) and (2) can now be rewritten as:

$$T_{magn} = T_{l,mech} + T_{l,fe} + T_{mech} = C_m * \Phi * I_a \quad (7)$$

$$V_a = C_m * \Phi * \omega_m + R_a * I_a + 2 * V_{br} * \frac{T_{magn}}{|T_{mech}|} \quad (8)$$

where T_{mech} and T_{magn} stand for the mechanical motor torque and the torque excited by magnetic forces (except for the torque corresponding with the iron losses) respectively.
In these equations three unknowns appear, viz. Φ, I_a and V_a, if one takes ω_m as known, thus a third equation must be found to solve the problem.
The speed of the motor can be controlled varying either the armature voltage or the field current or both. In the armature voltage control area the field current is held constant at its nominal value, which, if the armature reaction is neglected is given by the expressions:

$$C_m * \Phi = C_m * \Phi_o \text{ or } I_f = I_{f,0} \quad (9)$$

In the case of field control the armature voltage is equal to the total battery voltage and the field current is varied. In this situation one obtains:

$$V_a = V_{bat} \quad (10)$$

With these equations it is possible to calculate the power flow through the DC-motor both in driving and in regenerative braking conditions.
If the separately excited DC-motor is driving the vehicle the motor efficiency can be written as:

$$\eta_{m,m} = \frac{T_{mech} * \omega_m}{I_a * V_a + I_f * V_f} \quad (11)$$

During regenerative braking conditions defined by a net current flow back into the batteries

$(I_a * V_a + I_f * V_f < 0)$ the motor efficiency is described by:

$$\eta_{m,g} = \frac{I_a * V_a + I_f * V_f}{T_{mech} * \omega_m} \qquad (12)$$

There is a small operating area, in which the DC-machine dissipates some power to overcome the internal losses. During this operation the mechanical input power partially meets these power losses so that supplementary electric power is required

The battery charging and discharging model

When a battery is discharged or charged with constant current during a period Δt, the change in state of charge (S) can be calculated with the formulas [1]

$$\Delta S_d = \frac{I_d \Delta t_d}{C_5} \left(\frac{I_d}{I_5}\right)^{p-1} \qquad (13)$$

$$\Delta S_c = \frac{I_c \Delta t_c}{Q_d} f(1 - S) \qquad (14)$$

where C_5 = capacity at 5 hr rate
Q_d = net discharge
f = charge efficiency
p = exponent value in the Peuckert equation ($I^p * t$ = constant)

The subscripts c, d refer to charge respectively discharge.

In order to predict at any time during drive cycle operation the capacity that is available for discharge with current I_d, the state of charge is computed with eq. (15) taking into account regenerative charging:

$$S = 1 - \frac{Q}{C_5} \left(\frac{I_d}{I_5}\right)^{p-1} + \frac{\Sigma(fI\Delta t)_{charge}}{C_5} \qquad (15)$$

Q = total charge withdrawn.

The charge efficiency f ($0 \leq f \leq 1$) depends on the state of charge of the battery and the charging current. f was determined for a 6V EV battery (Varta 240-15) by simultaneous measurements of O_2 and H_2 gas evolution during charging at constant current at t = 27 ± 3°C. Figure 4 shows the charge efficiency for same currents.
These data were used to obtain charging current-voltage curves at constant state of charge.
Figure 5 represents these E - I characteristics, together with the curves that were established for discharge.

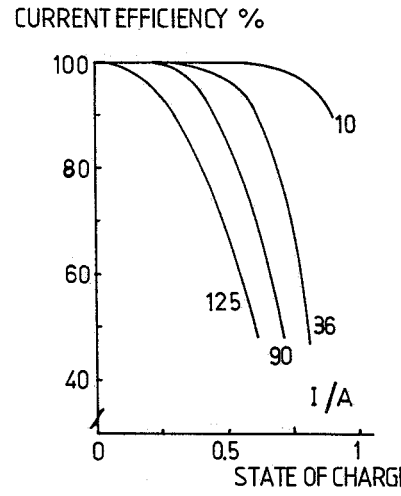

Fig. 4. Current efficiency during charging as a function of state of charge.

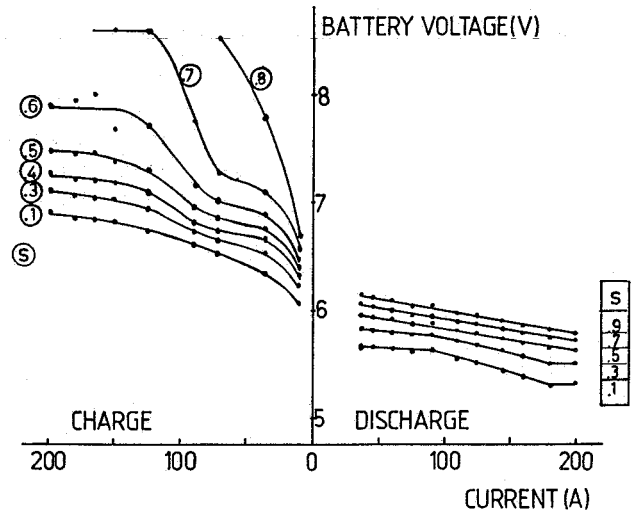

Fig. 5. Current-voltage characteristics at constant state of charge (6V battery).

The voltage time behaviour of the battery during discharge with a drive cycle and the decrease in state of charge were calculated on the basis of the data of figure 5. The results were compared with experimental data, measured while the battery was subjected to such discharge. The power requirements of the cycle were calculated for the Eindhoven Electric Car assuming constant efficiency of components [1].
Many deep discharge experiments were performed with the THE duty cycle, which is a non-idealized power profile of 1200 s and was described in [1].
After $4\frac{1}{3}$ hr discharge with 13 THE cycles the state of charge was found to be S = 0.18 ± 0.03 (with respect to C_5). This was in excellent agreement with the predicted value s = 0.18. The charging efficiency during this type of cycle appeared to be >90%.

The performance of the battery in terms of voltage

time curves was tested with the SAE J 227 D and the ECE-15 cycle. Here a good agreement was observed between the calculated and measured voltage during discharge, but the voltage during regenerative charging was considerably lower than the predicted value, as depicted for the SAE J 227 D cycle in figure 6. (dashed line).

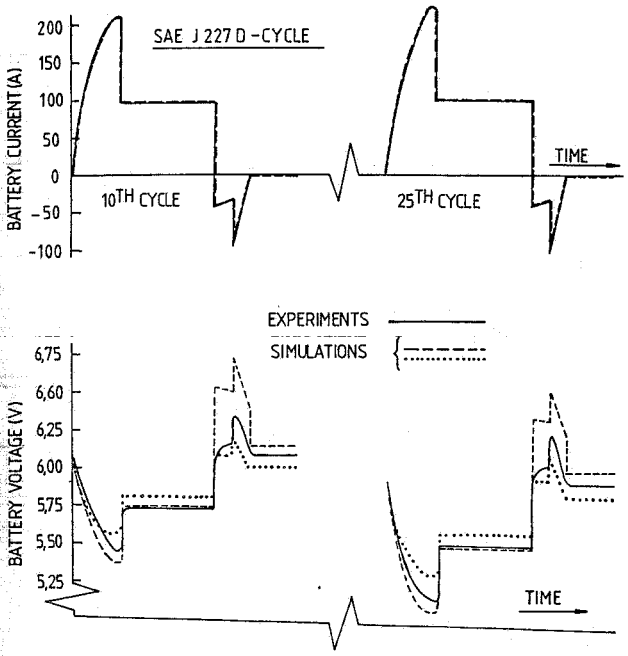

Fig. 6. Comparison of measure and calculated battery current and voltage.

Single pulse experiments with pulse duration up to 30 s showed that this discrepancy is due to the difference in battery voltage during continuous and short duration operation. For low state of charge the voltage reaches the value that is obtained during continuous operation after about 30 s both during charging and discharging. For high state of charge however the battery voltage during charging is considerably lower than the value obtained during continuous charging and differs after 30 s about 10%. Simular behaviour was noted by Schleuter [2] during measurement of the activation potential. These delay times exceed the duration of the varying pulses of drive cycles. Consequently for the prediction of the voltage behaviour during such discharge operation, instantaneous E - I - S characteristics are required as shown in figure 7. A fair approximation for these curves was obtained by presenting the charge and discharge curves as constant s lines extending from the stationary E - I

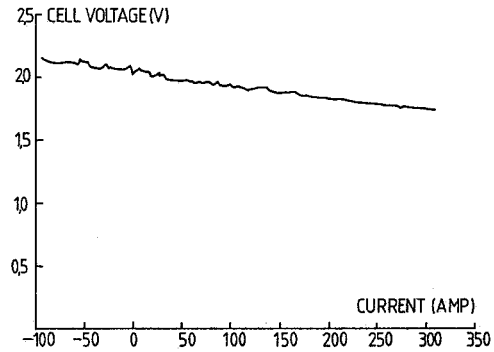

Fig. 7. Cell voltage during a driving cycle in dependence on current.

discharge regime into the charging regime: i.e. to assume constant total resistance for both discharge and charge. The calculated performance of the battery agrees then within 2% with the experimental curves as evidence by the dotted line in figure 6 (dotted line).

The simulation program

The characteristics of other driveline components, such as the mechanical transmission, and the controller and the road-load conditions have been described earlier. [3]

The equations describing the battery and the motor can be linked together, so that an expression is obtained, in which the battery voltage and current both appear as a function of the motor characteristics and the battery characteristics as given in previous chapters of this paper and as a function of the motor load.

Normally the computer input data are

- vehicle parameters and
- a driving cycle where the vehicle speed is given as a function of time.

The output data can be the power flow, energy-use and -losses at any point or device in the total drive line, and of course vehicle speed, distance covered etc.
As for the termination criterium there is a choice between a number of duty cycles and a minimum cell voltage, where the battery is declared to be fully discharged.

In figure 8 the flow-chart has been given, representing the modulus of the simulation program in a logical structure.

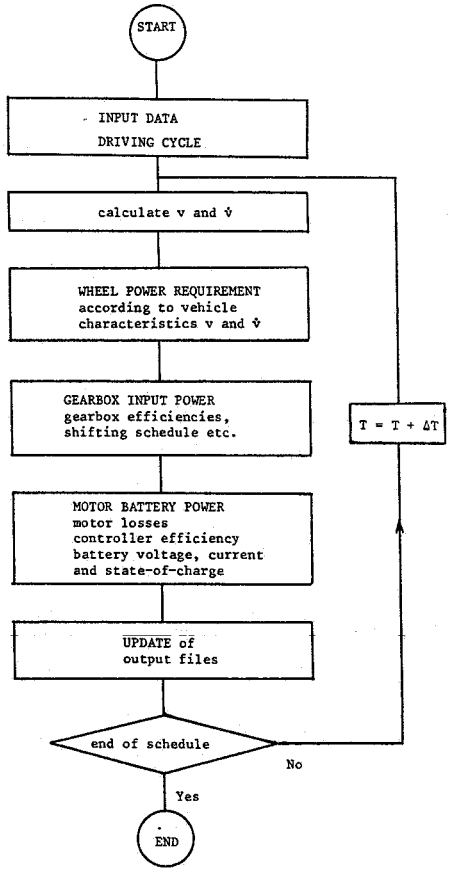

Fig. 8. Flow chart of the simulation program.

Experiments compared with simulations

Experiments with the Eindhoven Experimental Electric Vehicle, which is in fact a modified Volkswagen Golf, described in [4], were carried out in the road. This vehicle has been fitted out with measuring equipment so that:

- the flow of electric energy from the 120V battery pack to all energy consuming devices
- the electro-mechanical torque in the DC-motor and the mechanical torque in the cardanshaft to one of the driven frontwheels.
- the motor and vehicle speed

can all be determined in detail.
These measurements enable a thorough look into the energy management in the total drive train.

In figure 9 the recorded on-the-road speed profile is given. This speed profile resembles that of the SAE-Metropolitan cycle, apart from the duration which was extended from 130 to 210 seconds. This measured speed profile was used in the simulation calculations.
The momentary transmission efficiencies (fig. 10) result from these calculations.
In figure 11 the comparison can be seen between the calculated and the actually measured data for the battery voltage and current during the duty cycly

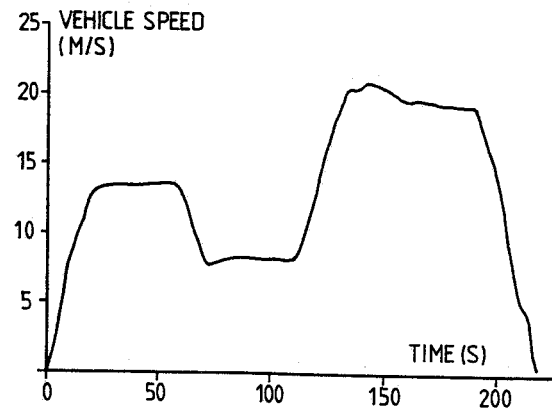

Fig. 9. Speed profile.

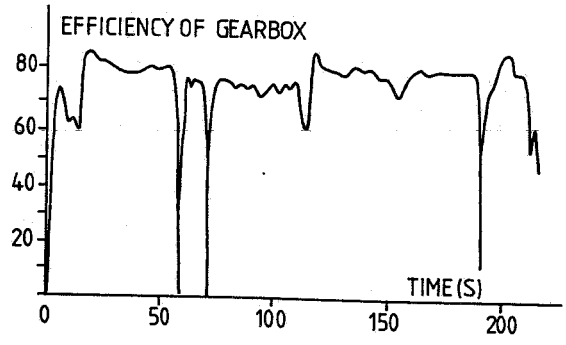

Fig. 10. Variable efficiency of mechanical transmission.

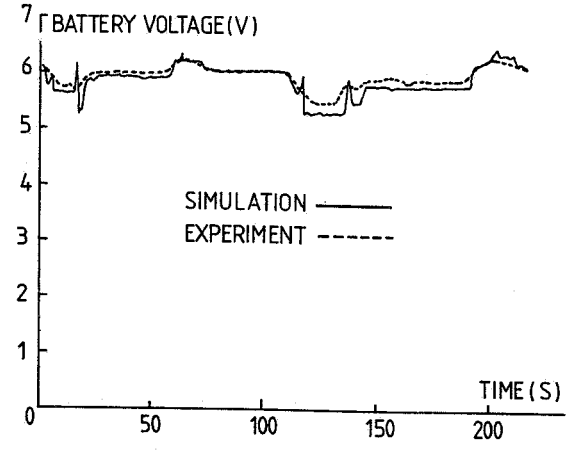

Fig. 11. Course of battery voltage.

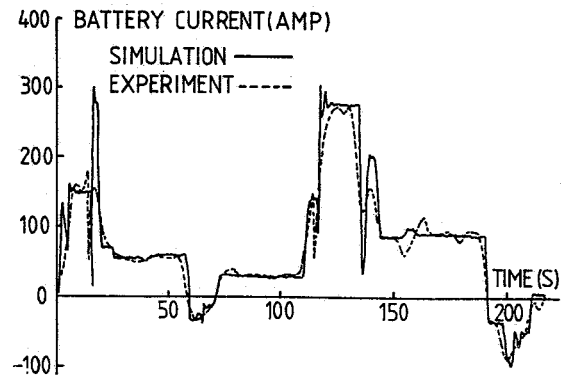

Fig. 12. Course of battery current.

given in figure 9. Here a very good agreement is found between the values that were estimated in such different ways. The same measured voltage and current data were used in fig. 7 in order to find voltage-current relations for load-acid batteries during exposure to a driving cycle.

Conclusions

Calculations based on load dependent efficiency characteristics of drive train components prove to give an adequate insight into the energy management in an EV. In this way battery voltage and current during arbitrary driving cycles can accurately be predicted. Hence is seems possible to estimate in advance the total charge which can be drawn from a known load acid battery in a road vehicle under normal traffic conditions.

Literature

1. W. Visscher and L.A.M. van Dongen
Battery State of Charge Model for Driving Cycle Operation.
Drive Electric Amsterdam '82.
Amsterdam, Oct. 1982.

2. W. Schleuter
Thesis Aachen 1982.

3. L.A.M. van Dongen, R. van der Graaf, W.H.M. Visscher
Theoretical Prediction of Electric Vehicle Energy Consumption and Battery State-of-Charge During Arbitrary Driving Cycles.
EVC-Symposium VI, Baltimore Oct. 1981.

4. L.A.M. van Dongen, R. van der Graaf
The Eindhoven Experimental Electric Vehicle: Vehicle design and drive train.
Drive Electric Amsterdam '82.
Amsterdam, Oct. 1982